Thermal Analysis of an Evacuated Tube Solar Collector using a One-end Stainless Steel Manifold for Air Heating Applications under Diverse Operational Conditions

Zaphar, Saifullah
School of Renewable Energy and Efficiency, National Institute of Technology, Kurukshetra

Chandrashekara M
Department of Mechanical Engineering, National Institute of Technology, Kurukshetra

Verma, Gaurav
Department of Electronics & Communication Engineering, National Institute of Technology, Kurukshetra

https://doi.org/10.5109/6792885

出版情報：Evergreen. 10 (2), pp.897-911, 2023-06. 九州大学グリーンテクノロジー研究教育センター
バージョン：

Thermal Analysis of an Evacuated Tube Solar Collector using a One-end Stainless Steel Manifold for Air Heating Applications under Diverse Operational Conditions

Saifullah Zaphar[1,*], Chandrashekara M[2], Gaurav Verma[3]

[1]School of Renewable Energy and Efficiency, National Institute of Technology, Kurukshetra, India

[2]Department of Mechanical Engineering, National Institute of Technology, Kurukshetra, India

[3]Department of Electronics & Communication Engineering, National Institute of Technology, Kurukshetra, India

*Author to whom correspondence should be addressed:

E-mail: Saifullah_61900089@nitkkr.ac.in

(Received March 16, 2023; Revised May 8, 2023; accepted May 12, 2023).

Abstract: The thermal performance of one-ended stainless-steel manifold-based evacuated tubes, solar air collectors, using air as the working fluid, is the subject of an experimental investigation carried out in the winter season at Glocal University, Saharanpur, India [30^0 17' (latitude) North and 77^0 38' (longitude) East]. Nine evacuated tubes with directed inner tubes of varying diameters are placed in a one-ended stainless-steel manifold to form the solar collector. The input air passes through the directed inner stainless tubes inside the evacuated tubes due to forced convection. In this experiment, hot air is produced in evacuated tubes, gathered in the main header manifold, and released through the output pipe. The airflow velocity, directional stainless steel tube diameter, air mass flow rate, and solar intensity influence the air temperature exiting the outlet. At a solar intensity of 616.2 W/m^2, the highest temperature measured is 90.5 ^{0}C, and the maximum temperature difference between the exit air and the input air was measured to be 62.5^0C at a flow rate of 4.58 kg/h in a stainless-steel tube with a 20 mm diameter and 1.27 meters length.

Keywords: evacuated tubes, solar air collector; directional inner stainless-steel tubes; forced convection; airflow; solar intensity, thermal performance

1. Introduction

Renewable Energy, particularly solar Energy, is crucial in reducing reliance on the traditional energy source. The essential characteristics of solar Energy are its endless supply, pure energy source, lack of moving components, and Silent operation[1)]. The rigorous research studies carried out by numerous researc hers are discussed here. Researchers[2-6)] have investigated a thermal performance analysis at different operating conditions. Thermal performance and cost-effectiveness are essential when selecting the solar collector[7)]. Ge et al.[8)] studied that evacuated tube collectors are far more efficient and effective in capturing solar Energy than conventional absorber field collectors.

A literature survey on evacuated tube solar collectors indicates that significant effort has already been made in research and development. The evacuated tube collector has been used to heat water for a long time but never to heat hot air. Kumar et al.[9)] performed experiments on the thermal analysis of evacuated tube collectors. The collector had an inner fitted Aluminium tube. By utilizing the different lengths of the tube and analyzing by increasing the tube length, the temperature difference also increases at a low air flow rate. As per the experimental investigation of the vacuum tube, it reduces the heat loss to the environment, reduces gaps between tubes, increases absorber area, and increases the solar radiation received by the evacuated tube[10)].

S. Kumar et al.[10)] studied experimental results that evacuated tube collector shows that the outlet temperature is very high and has a better energy-saving ability. Zubriski et al.[11)] studied the efficiency of evacuated tube collectors under various operating conditions, such as the angle of inclination based on design and installation. The result shows that vertical installations were more efficient than other designs and suggested that increasing the mass flow rate and volume flow rate will cause an increase in collector efficiency. A measure of system effectiveness will be more appropriate for performance analysis. Mehla et al.[12)] experimentally investigated phase change material that the system works better in off-shine hours. Zambolin et al.[13)] studied the performance comparisons

with and without the reflector effect. An optical efficiency increase of 66% higher compared to the optical efficiency without compound parabolic concentrators. Felińsk et al.[14] compared simple evacuated tube collectors to evacuated tube collectors containing heat pipe in which the paraffin is used as a working fluid heat pipe. A paraffin-filled heat pipe increased the total heat output by about 45-79%[15]. Chopra et al.,[16] studied the thermal analysis of an evacuated tube solar collector with and without a heat pipe system. The nanocoated heat pipe could handle higher heat flux[17]. They concluded that the heat pipe's condenser area's small section results in less helpful heat transfer; hence there is room for improvement by lengthening the condenser area. Singh et al.[18] did an economic analysis using evacuated tube solar collectors assisted with greenhouse driers and found 39% of electrical energy savings with a minimum payback period.

Kim & Seo[19] did the numerical and experimental thermal performance of evacuated tube solar collectors and investigated that the collector temperature and efficiency depend upon the absorber area. Munim & Bidyut[20] explore energy resources with skillful utilization. Paul. B et al.[21] focus on the energy performance of the storage system by PCM. The proposed nanofluid exhibits a superior increase in fluid flow behavior than the base fluid water[26]. An innovative solution must be commercially viable for household and industrial use[27]. When compared to the straightforward ETSAC, ETSC with helical inserts has been found to perform better and produce greater air temperatures[28]. The temperature increases were discovered to be flow rate independent but sensitive to changes in sun intensity[29].

Evacuated tubes have been experimentally studied by many researchers that are interested in heating water and air with an intermediary fluid. Without using intermediary fluid, the current experiment intends to produce hot air at variable flow rates by varying the diameter of directional inner steel tubes with a consistent length of 1.27 meters. Thermal efficiency and output temperature differences will be monitored throughout the day. At Glocal University in Saharanpur, Uttar Pradesh, India, the experimental setting is 30^0 17' (latitude) North and 770 38' (longitude) East. Solar intensity depends upon sun rises, longitude, and latitude of place with an angle of inclination of the evacuated tube[25].

1.1 Scope & Necessity of the present work

The mandate for solar Energy is rising to meet future energy requirements in various industries in the ancillary of fossil fuels, which reduces global warming. In both the home and industrial segments, evacuated tube solar collectors (ETSCs) use solar radiation to heat air, water, and dry agricultural products. The enormous scope in food processing industries for drying food commodities with suitable chamber design using effective ETSCs.

1.2 The objective of the experimental work: The current experiment's objective is to generate hot air at different flow rates by using the 20mm diameter of directional inner steel tubes with a uniform length of 1.27 meters and measuring the maximum temperature, difference in output temperature & thermal efficiency throughout the day. And Finally, compare the experimental results of the different solar collectors based on the previously obtained results. The experimental setup is installed at Glocal University, Saharanpur, UP India [30^0 17' (latitude) North and 77^0 38' (longitude) East]. Data were collected from 11th November to 20th November 2022.

Weather data[31]

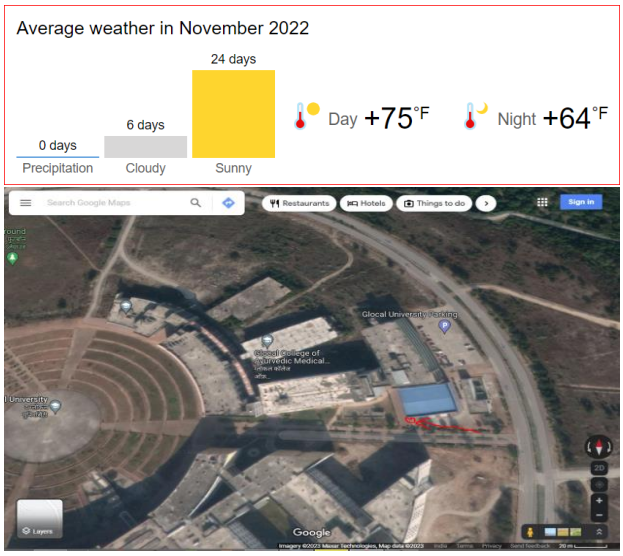

Fig. 1 location of the project is indicated with the red arrow (Google Maps) showing the exact location of the experiment Google Maps, 2023[30].

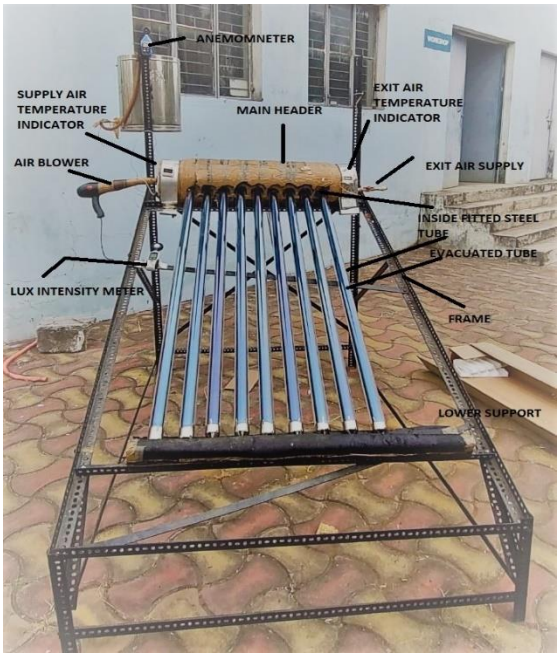

Fig. 2: Experimental Set up of ETSAC

2. Experimental Setup

The thermal performance of an evacuated tube solar air collector is examined in this experiment using directed inner stainless-steel tubes of varying diameters. Fig. 2. is a snapshot of the experimental setup. The experimental setup had nine glass evacuated tubes measuring 1.5 meters long. The outer glass and Absorber tubes had diameters of 0.047 and 0.037 meters, respectively. The insulated main manifold channel, which has a square bar in the middle and is 0.860m long, is where the open ends of evacuated tubes are linked. A blower with a regulator blows air into the evacuated tubes and regulates the air flow rate.

The experimental setup consists of the following parts:

- Evacuated tube
- Inner Square bar manifold channel fitted in main manifold header
- Frame

- **2.1 Evacuated tube** borosilicate glass tubes with a vacuum of 5 x 10^{-2} Pa between them. The outer tube is luminous to reduce reflection, and the inner tube is coated (Al-/Al).

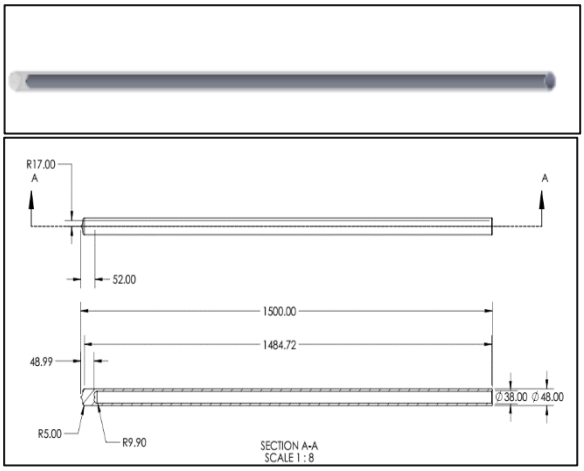

Fig. 3: Evacuated Tube

Table 1 Thermophysical properties of evacuated solar tube collector[22)]

Material	**Parameters**	**Value**
Glass Tubes: (Borosilicate)	Normal Reflectivity	0.04
	Density	2.23 g/cm^3
	Maximum Temperature	430 ^{0}C
Outer Glass Tube	Diameter(external)	47 mm
	Thickness	1.2 mm
	Transmissivity	0.92
	Emissivity	0.9
Inner Glass tube	Diameter(external)	37 mm
	Thickness	1.2 mm
	Transmissivity	0.9
	Emissivity(outward)	0.35
	Emissivity (Inward)	0.08
Stainless steel tube (SS-304)	Conductivity Density	16.2 W/mK 7.93 Kg/m^3
	Emissivity	0.54-0.63
	Diameter (external)	20 mm
	Thickness	2 mm
	Stainless steel tube Length	1270 mm
Evacuated tube	Evacuated Tube length	1500 mm
Solar collector	The angle of inclination of the tube	30^0

2.2 Inner Square bar manifold channel fitted in the main header

Fig. 3 depicts the square bar inner manifold channel used in this design. It comprises a square bar made of stainless steel with one end closed and is inserted within the circular header manifold with its edges aligned in the middle. The square bar is drilled with nine 20 mm and 10 mm circular holes concentric with circular header manifold holes. The holes have an internal thread in which a 20 mm and 10 mm diameter mild stainless-steel pipe can be fitted in the nine holes. The purpose of this square steel bar is to supply the air and pass through the inner stainless-steel tube fitted inside the evacuated tube. The inner stainless-steel tube directs the airflow into the evacuated tube.

2.3 Frame

It comprises a slotted steel bar in which a header can be fitted into a frame. Additionally, the frame is built so that the evacuated tube can be securely fastened in the header and lower support.

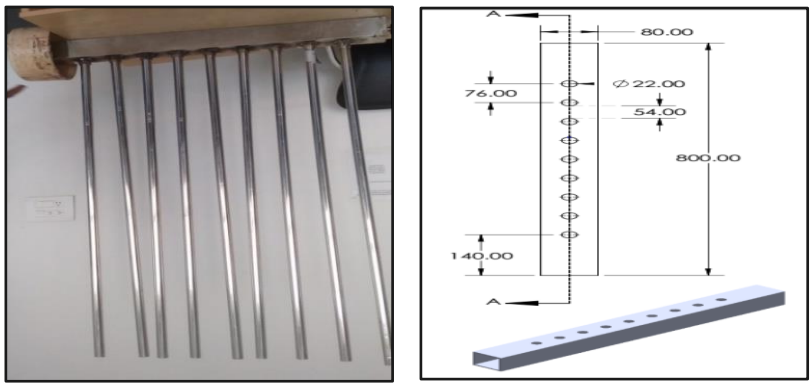

Fig. 4: Shows the Inner Square bar manifold channel fitted in the main header

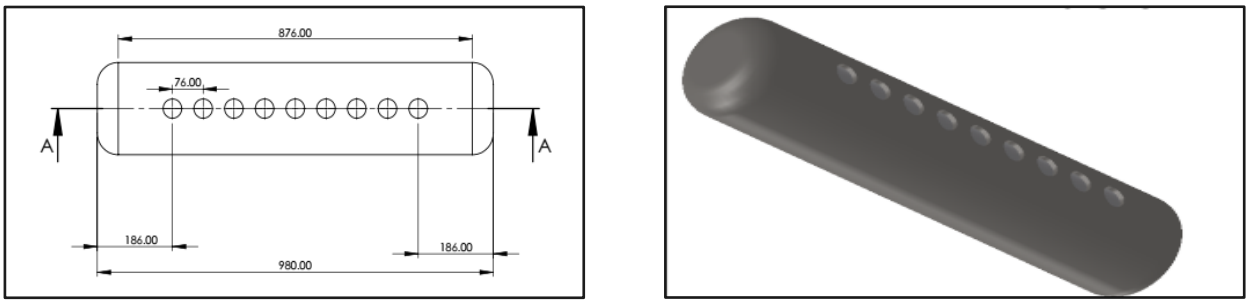

Fig. 5: Shows the main header with 2-d & 3d View

2.4 Measuring Instruments

Various important measurement data have been recorded through different instruments, such as temperature at various points by digital temperature indicators, solar intensity data by solar intensity meter, air flow rate by an anemometer, atmospheric temperature and humidity level by a hygrometer, etc.

Different parameters measured in this study include:

- Temperature,
- Solar intensity
- Air flow rate and air velocity
- Ambient temperature and humidity

Temperature measurement, LCD corded digital temperature of the model (AP-IS11A001) is used, whose temperature range is -50^0 C to 110^0 C with an accuracy level of ± 1 ^{0} and resolution of 0.1.

Solar Intensity meter (Lux Meter) measures the solar radiation of the model NAAFIE Meco -930P with an accuracy level ± 5% of range:0 ~ 200,000 lux and resolution 0.1 lux operated by 9V battery with auto power off. .

Air Flow Rate and air velocity, To measure the air velocity, a digital mini anemometer of a model (AVM-01) is used to measure the air velocity at the pipe's exit. Air Velocity measurement up to 30m/sec &Air Temperature -10 to 50 Degree C.

Ambient temperature and humidity, model HTC-1 Digital LCD Hygrometer and thermometer are used to measure the ambient temperature and humidity level. Temperature range -50^{0}C to 70^{0}C with temperature accuracy level ±1°C, humidity range 20% RH to 90%RH with accuracy level ±5%.

Table 2 Design parameters of manifold channel and main header

Design parameters	Design Value (m)	Design material
Inner Manifold Channel: Rectangular Square bar hollow, ((LxWxH) The Thickness of Stainless steel, (ts)	 0.8 x 0.08 x 0.08 0.055	Stainless steel (304 Grade 2B)
Header main manifold (length & diameter) Thickness of pipe, (tp)	 0.96 & 0.02 0.03	CPVC Pipe
Main header insulation thickness, (ti)	0.025	PUFF
Silicon seal(ϕ)	0.04	Silicon rubber

S.No	Parts
1.	Frame
2.	Header manifold
3.	Inner Square manifold channel
4.	Heat Resistant rubber seal
5.	Exit Air pipe
6.	Inner Stainless-steel Tube
7.	Evacuated Tube
8.	Evacuated tube holder
9.	Air Blower,

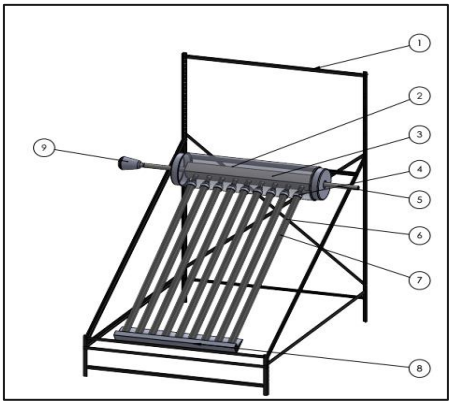

Fig.6: Schematic diagram of ETSAC with all parts

2.5 System Operation:

Fig. 7. shows a two-dimensional schematic of an evacuated tube solar air collector setup. The intake air can travel through the inner square pipe with the other end closed in this operation. The inner square pipe includes nine threaded holes of 10 mm and 20 mm diameters and 1.27 meters in length that can hold stainless steel tubes of two different diameters.

The forced input air supply to a square steel pipe from it directs into the evacuated tubes via inner-fitted stainless-steel tubes. It acquires heat from solar radiation and subsequently departs through the outer circular pipe of the manifold channel owing to the thermosyphon effect. The stainless-steel tube's function is to separate the incoming cold air from the hot air and to facilitate heat transfer through the evacuated tubes. Moreover, stainless steel tube serves as an absorber to take up solar radiation's heat energy.

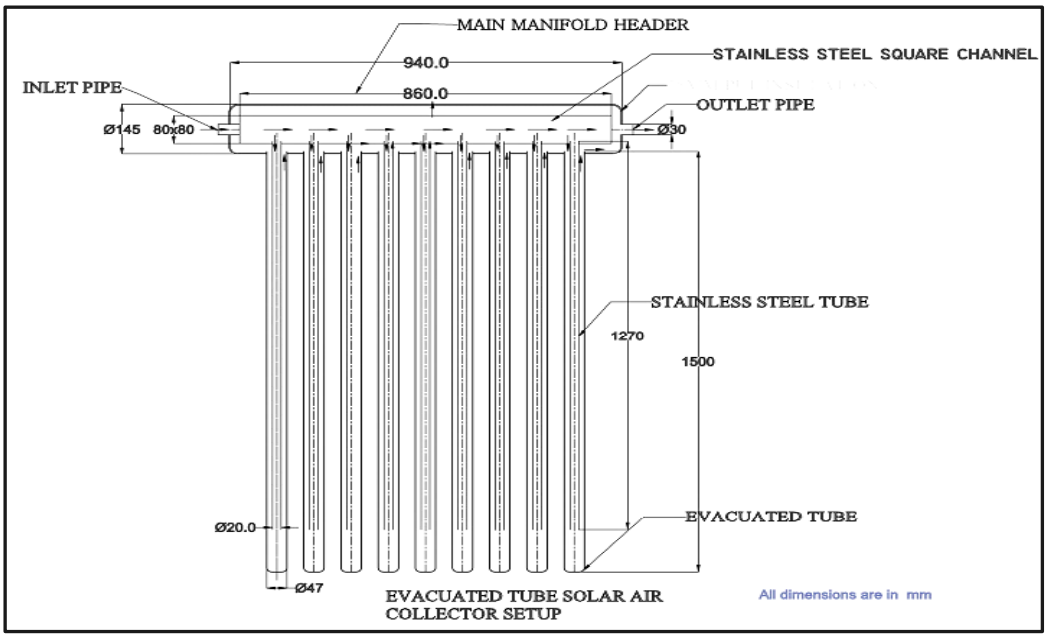

Fig. 7 Schematic diagram of ETSAC with stainless steel manifold channel

3. Thermodynamics performance analysis of ETSC

Governing Equations,[23)]

Few assumptions are considered for a simplified collector analysis.

- Steady-state heat transfer process
- No heat loss from stainless steel tube
- Convective heat transfer inside the evacuated tube is neglected

$$\frac{G_{abs}}{G} + \frac{G_{ref}}{G} + \frac{G_{tr}}{G} = \frac{G}{G} \quad (1)$$

$$\propto + \rho + \tau = 1 \quad (2)$$

3.1 Transmissivity of the evacuated glass,[23)]

$$\propto + \rho + \tau = 1 \quad (3)$$

But the evacuated tube is not opaque $\rho = 0$

$$\tau = 1 - \alpha \quad (4)$$

From Kirchhoff's law,

- Radiation by a blackbody

$$G = E_b(T) = \sigma T^4 \quad (5)$$

- Radiation absorbed by a body

$$G_{abs} = \alpha G = \alpha\sigma T^4 \quad (6)$$

- Radiation emitted by a body

$$E_{emit}(T) = \varepsilon\sigma T^4 \quad (7)$$

Thermal equilibrium

$$A_s\varepsilon\sigma T^4 = A_s\alpha\sigma T^4 \quad (8)$$

$$\text{Thus } \varepsilon(T) = \alpha(T) \quad (9)$$

3.2 Heat transfer coefficient

The overall heat transfer coefficient between the glass tube and the ambient air is given as[15]

$$U_{a-g} = h_{c,\infty} + h_{r,g-\infty} \quad (10)$$

$$h_{c,\infty} = 5.7 + 3.8v_\infty \quad (11)$$

$$h_{r,g-\infty} = \in_g \sigma\left(T_\infty^2 - T_{go}^2\right) \quad (12)$$

$$U_{a-g} = 5.7 + 3.8v_\infty + \in_g \sigma\left(\mathrm{T_{ig,o}} - \mathrm{T_{og,i}}\right) \quad (13)$$

The radiation heat transfer coefficient between the absorber surfaces of stainless steel and the glass tube,

$$h_{r(ig,o-og,i)} = \frac{\sigma\left(T_{ig,o}^2 + T_{og,i}^2\right)\left(T_{ig,o}^2 + T_{og,i}^2\right)}{\frac{D_{og,i}}{D_{ig,o}} \times \frac{1-\in_{ig}}{\in_{ig}} + \frac{1}{F_{og-ig}} + \frac{1-\in_{og}}{\in_{og}}} \quad (14)$$

Overall heat transfer coefficient between the surface of the stainless-steel tube and the water in the tube,

$$U_{w-ss} = \frac{1}{\frac{D_{os}}{D_{is}} \times h_c + \frac{D_{os}}{2k_m} \times \ln\left(\frac{D_{os}}{D_{is}}\right)} \quad (15)$$

3.3 Energy balance on the inner surface of the stainless-steel tube

$$= \frac{2\pi k_g l\left(T_{ig,o} - T_{ig,i}\right)}{ln\left(\frac{r_{ig,o}}{r_{ig,i}}\right)} = h_{c(is)} A_s\left(T_s - T_w\right) \quad (16)$$

3.4 Collector efficiency,[24]

To assess the effectiveness of an evacuated tube solar air collector, we must ascertain the thermal efficiency of the collector. By dividing the useful heat energy input by the useful heat energy input in terms of solar radiation on the ETSAC per unit area, one can determine the thermal efficiency of the collector. The collector efficiency depends on average sunshine hours and the clearness index.

$$\eta = \frac{\boldsymbol{Q_{out}}}{\boldsymbol{Q_{in}}}$$

The ETSAC is exposed to solar radiation from morning 9 am to evening 5 pm. During these hours, the evacuated tubes absorb solar radiation, heat energy is transferred from the inner tube to the air, and the air gets heated further,

The heat energy input is the solar radiation from the evacuated tube collector area.

Mathematically,

$$\mathrm{Q_{in}} = \mathrm{I_{eff}} A_c \quad (17)$$

Where,

$$\mathrm{I_{eff}} = \alpha\tau \mathrm{I} \quad (18)$$

$$\mathrm{Q_{out}} = \text{Heat gain by the air} = \dot{m}_a\, \mathrm{C_{pa}}\left(\mathrm{T_{air\ out}} - \mathrm{T_{air\ in}}\right) \quad (19)$$

Where A_c= Collector surface area of one tube, m^2 (Ma et al., 2010) is given by

$$A_c = 2DL_E \quad (20)$$

$$\eta = \frac{\dot{m}a\ Cpa\ (Tair\ out - Tair\ in)}{\alpha\tau IAc} \quad (21)$$

4. Experimental Results and Discussion

This experimental setup aims to heat the air under various operational and geometrical circumstances. The experiments were conducted in clear weather conditions during the daytime in October and November 2022. The temperature during working hours often ranged from 18°C to 28°C, but on rare occasions, it reached 30°C. The experiment ran from 9 am to 4:30 pm. The experiment was conducted for the following scenarios, and the outcomes were described via a graphic comparison.

Case 1: Evacuated tube with the stainless-steel manifold channel at directional inner stainless-steel tube diameter 20mm and length 1.27 meters at different air mass flow rates.

Case 2: Evacuated tube with the stainless-steel manifold channel at directional inner stainless-steel tube of diameter 10 mm and length 1.27 meters at different air mass flow rates.

Case 3: Evacuated tube with the stainless-steel manifold channel with no inner stainless-steel tube at different air mass flow rates.

4.1 Case 1: Evacuated tube with the stainless-steel manifold channel at a directional inner stainless-steel tube of diameter 20 mm and length of 1.27 meters at a different mass flow rate.

4.1.1 At a low flow rate of 4.58 (kg/h)

Fig. 8a and Fig.8b show that the air temperature differential in the ETSAC gradually rises due to an

increase in air residence time at a low flow rate of 4.58 kg/h with a 20mm stainless steel tube. The sun intensity is observed to be highest at midday. The temperature differential in the air is affected by sun intensity. The temperature difference grows as the solar intensity grows and reduces as the solar intensity decreases. At a sun intensity of 616.2W/m^2, the highest temperature differential in the air is 63^{0}C, and the maximum temperature reached is 90.5^{0}C.

As seen in Fig. 8c. after 2 pm, efficiency rises at a modest flow rate as sun intensity falls. This is due to the inverse intensity ratio at a constant airflow rate when the sun intensity is 158.96 W/m^2. The efficiency reaches its peak of 17.77%.

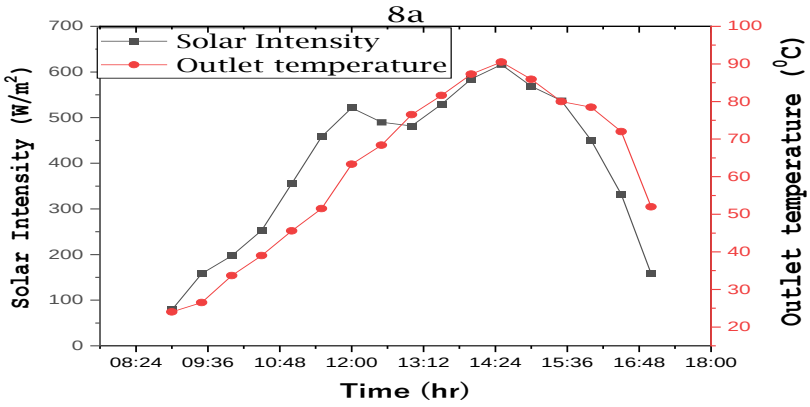

Fig. 8a: Day-to-day variation in outlet temperature and sun intensity at a flow rate of 4.58 kg/h using directed inner stainless-steel tubes 1.27 m long and 20 mm in diameter. Date 1st November 2022

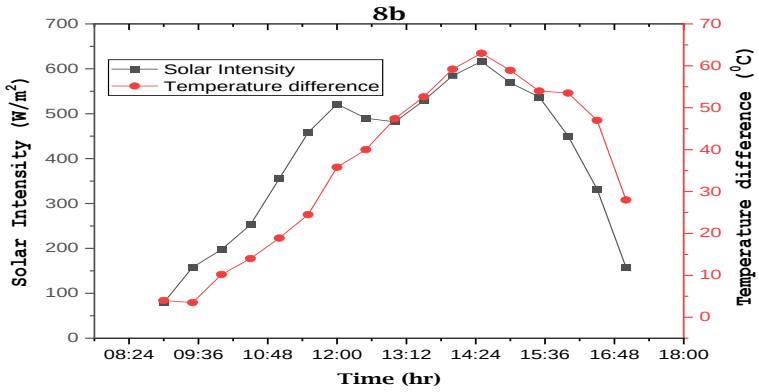

Fig. 8b: Temperature differential and sun intensity variations throughout the day at a flow rate of 4.58 kg/h using directional inner stainless-steel tubes 1.27 m long and 20 mm in diameter. Date 1st November 2022

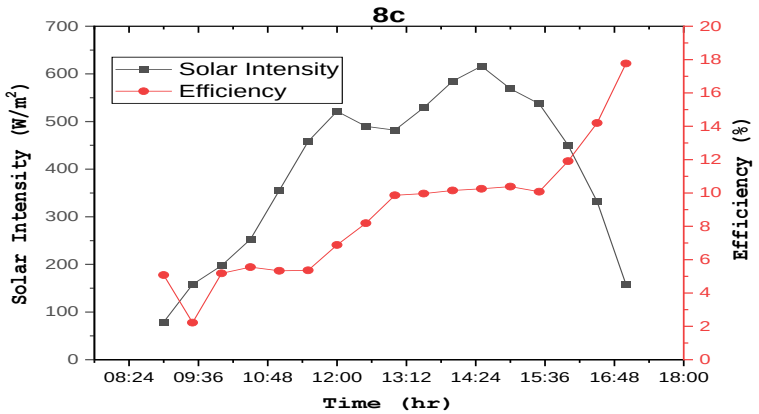

Fig. 8c: Efficiency and sun intensity variations throughout the day at a flow rate of 4.58 kg/h using directional inner stainless-steel tubes 1.27 m long and 20 mm in diameter. Date 1st November 2022

4.1.2 High flow rate: 15.14(kg/h)

As demonstrated in Fig. 9a. and Fig. 9b. increasing the air mass flow rate from 9.16 kg/h to 15.14 kg/h using a stainless-steel tube 20 mm in diameter and 1.27 meters in

length resulted in a drop in maximum outlet temperature and maximum temperature difference throughout the day.

The air retention period is shortened by increasing the air mass flow rate. The maximum air temperature difference with a solar intensity of 612.25 W/m^2 is 29^{0}C, while the maximum outlet temperature is 60^{0}C. As illustrated in Fig. 9c. the efficiency rises at a high flow rate as the airflow rate increases. A solar intensity of 165.9 W/m^2 achieves maximum efficiency of 28.97%.

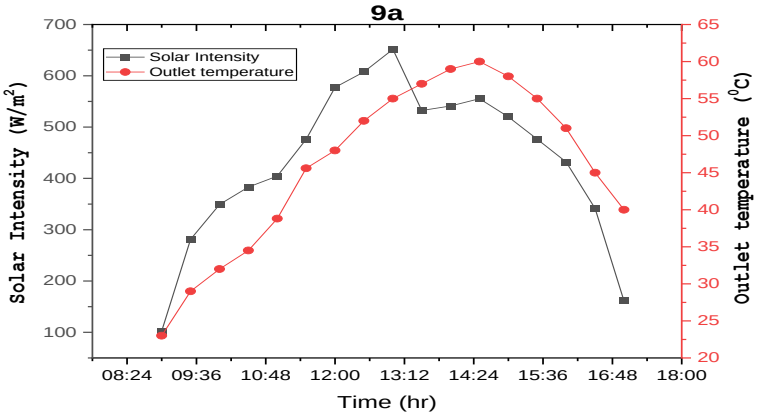

Fig. 9a: Demonstrates the daily variation in outlet temperature and sun intensity for a flow rate of 15.14 kg/h using directed inner stainless-steel tubes with a length of 1.27 m and a diameter of 20 mm. Date 2nd November 2022.

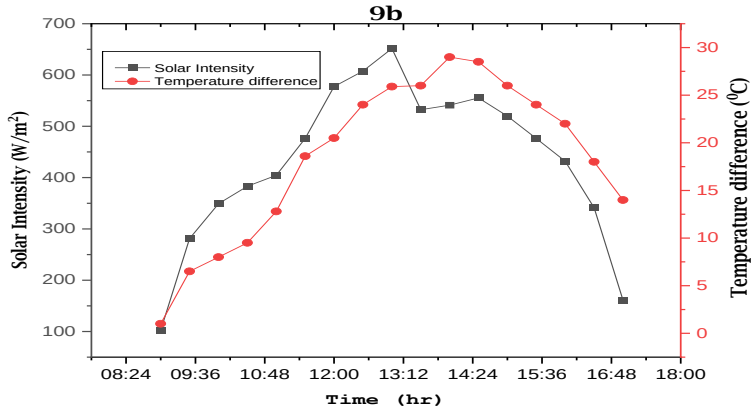

Fig. 9b: Illustrates the daily variation in temperature differences and sun intensity for a flow rate of 15.14 kg/h using directed inner stainless-steel tubes with a length of 1.27 m and a diameter of 20 mm. Date 3rd November 2022.

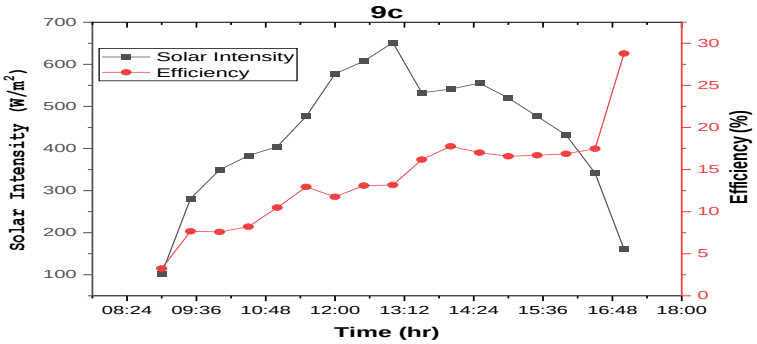

Fig. 9c: Shows the daily variation in efficiency and solar intensity using directed inner stainless-steel tubes with a length of 1.27 m and a diameter of 20 mm. Date 3rd November 2022

4.2 Case 2: Evacuated tube with the stainless-steel manifold channel at directional inner stainless-steel tube of diameter 10 mm and length 1.27 meters at different air mass flow rates.

4.2.1 Low flow rate 4.58(kg/h)

At a low flow rate of 4.58 kg/h, the temperature difference of air decreases from 63.9 ^{0}C to 48 ^{0}C,

when the diameter of the inner stainless steel tube changes from 20 mm to 10 mm at the same low flow rate, and the maximum temperature achieved decreases from

95.9 ^{0}C to 77.5 ^{0}C at the same condition, as shown in Fig. 10a. and Fig. 10b. This is because the air occupied inside the evacuated tube rises when comparing a 20 mm stainless steel tube to a 10mm stainless steel tube. As shown in Fig.10c. At a low flow rate, it is observed that the efficiency reaches the value of 14.9% at the solar intensity of 158.79 W/m^2.

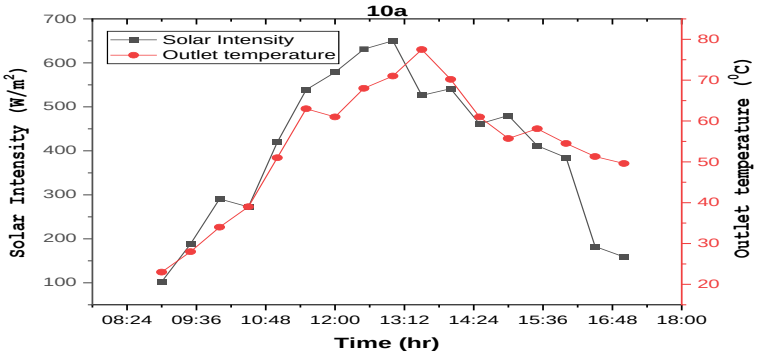

Fig. 10a: Shows the daily variation in outlet temperature and sun intensity for a flow rate of 4.58 (kg/h) with directed inner stainless-steel tubes that are 1.27 m long and 10 mm in diameter. Date 4th November 2022

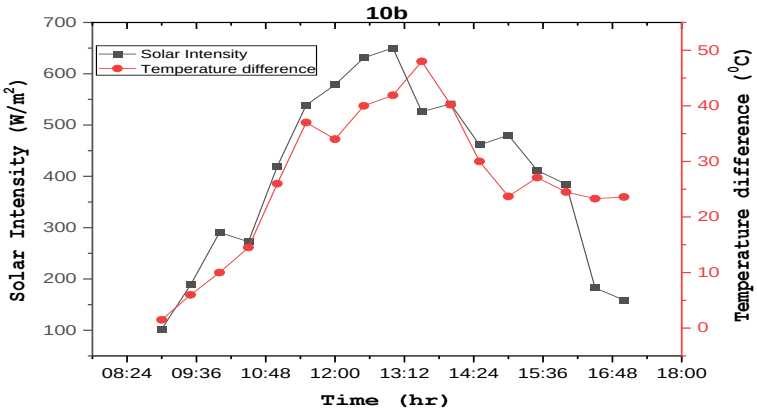

Fig. 10b: Shows the daily variation in temperature difference and sun intensity for a flow rate of 4.58 (kg/h) with directed inner stainless-steel tubes that are 1.27 m long and 10 mm in diameter. Date 4th November 2022

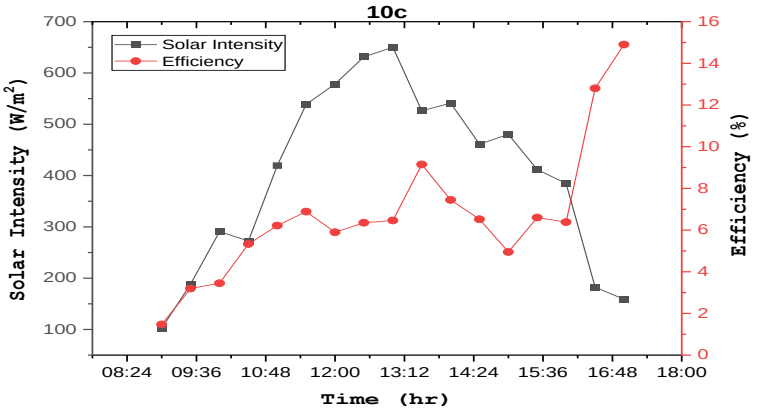

Fig. 10c: Shows the daily variation in efficiency and solar intensity using directed inner stainless-steel tubes with a diameter of 10 mm and a flow rate of 4.58 (kg/h). Date 4th November 2022.

4.2.2 High flow rate: 15.14(kg/h)

As demonstrated in Fig. 11a. and Fig. 11b. at a high flow rate of 15.14 kg/h with a 10 mm diameter stainless steel tube, the temperature differential and outlet temperature drop as the diameter of the stainless-steel tube and the mass flow rate of air increase. This is because the air retention time within the evacuated tube reduces, resulting in a decrease in the rate of heat transfer and heat gain input. In the case of a 10 mm diameter stainless steel tube, the maximum temperature difference and maximum output temperature drop to 32.6 ^{0}C and 61.7 ^{0}C, respectively.Fig.11c. Shows that at a high flow rate using

a stainless-steel tube of 10mm diameter, the efficiency improves as the flow rate of air increases. At a solar intensity of 241 W/m^2, it achieves maximum efficiency of 24.8%. Still, let's compare the findings to a 20mm steel tube diameter. In such a scenario, it is discovered that the efficiency. Temperature difference and output temperature produced with a 20 mm stainless steel tube are considerably more significant.

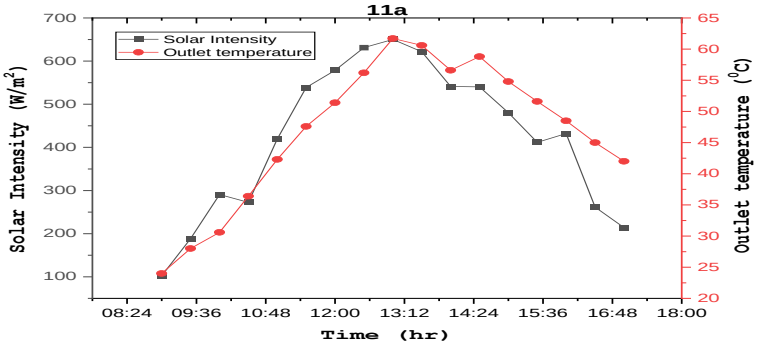

Fig. 11a: Shows the daily variation in outlet temperature and sun intensity for a flow rate of 15.14 kg/h using directed inner stainless-steel tubes with a length of 1.27 m and a diameter of 10 mm. Date 6th November 2022

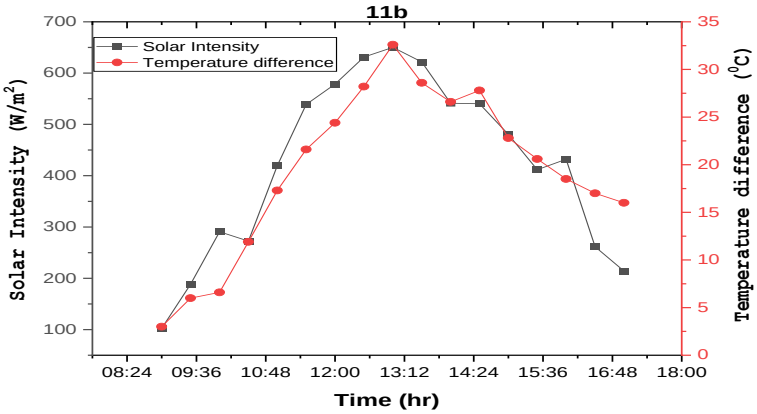

Fig. 11b: Shows how the temperature and the amount of radiation change during the day at a flow rate of 15.14 kg/h using directed inner stainless-steel tubes with a length of 1.27 m and a diameter of 10 mm. Date 6th November 2022.

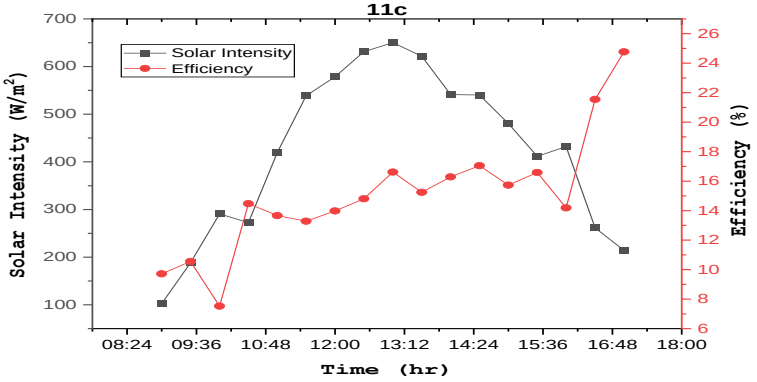

Fig. 11c: Shows the daily variation in efficiency and solar intensity using directed inner stainless-steel tubes with a length of 1.27 m and a diameter of 10 mm. Date 6th November 2022

4.3 Case 3: Evacuated tube with the stainless-steel manifold channel without an inner stainless tube.

4.3.1 Low flow rate:4.58 (kg/h)

Fig. 12a. and Fig. 12b. illustrate that at a low flow rate without a stainless-steel tube, the temperature difference and output temperature are smaller than in the previous two situations. In this scenario, the highest temperature difference at a low airflow rate of 4.58 kg/h is 36.7^{0}C at 621.73 W/m^2. In contrast, the maximum temperature difference at a low flow rate with a diameter of 20mm and 10mm stainless steel tubes is 63.9^{0}C and 48^{0}C, respectively. Also, the maximum outlet temperature in this situation of low flow rate is 64^{0}C, as opposed to 95.9^{0}C and 77.5^{0}C for stainless steel tubes with diameters

of 20mm and 10mm, respectively.
As demonstrated in Fig. 12c. at a low flow rate without stainless steel tubes, the efficiency is the lowest compared to the previous two examples since heat transfer retained inside the evacuated tube is lost to the surrounding environment. At a solar intensity of 261 W/m^2, the highest efficiency is 8.3%.

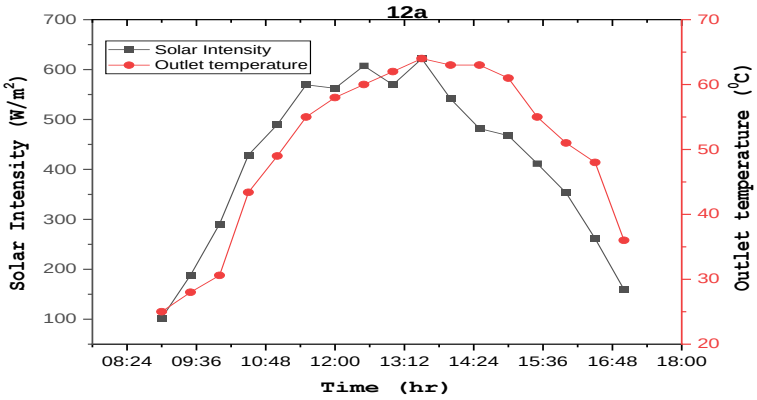

Fig. 12a: Shows the daily variation in outlet temperature and solar intensity for a flow rate of 4.58 kg/h. Date 7th November 2022

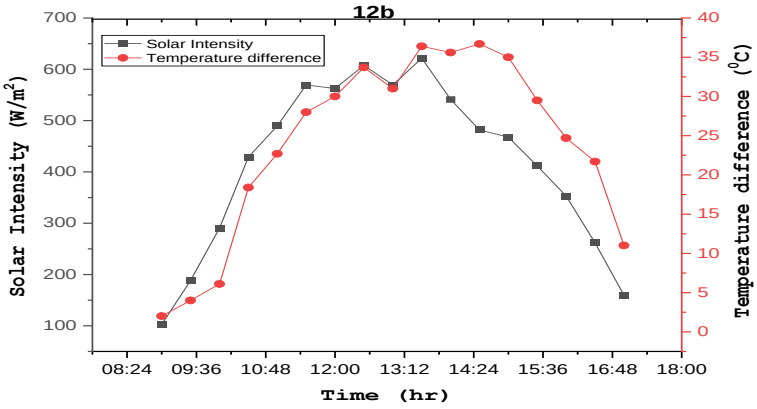

Fig. 12b: Shows how the sun intensity and differential temperature change during the day at a flow rate of 4.58 kg/h. Date 7th November 2022

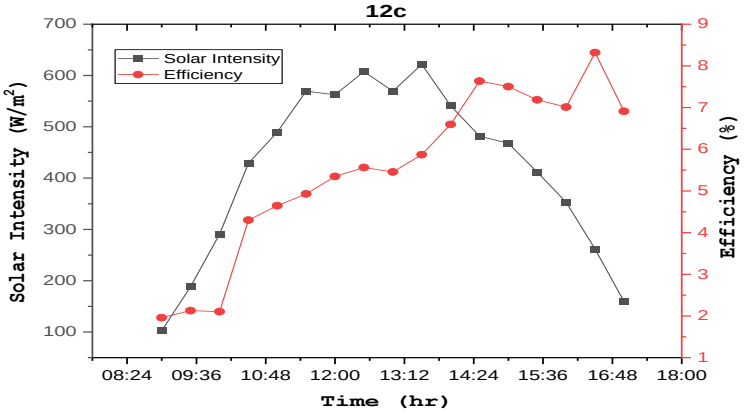

Fig. 12c: Shows the daily variation in efficiency and solar intensity at a flow rate of 4.58 kg/h. Date 7th November 2022

4.3.2 High flow rate, 15.14(kg/h)

Fig. 13a shows that at a high flow rate without stainless steel tube, the outlet temperature lowers, and the maximum outlet temperature approaches 51^{0}C, which is lower than the previous two examples. This occurs due to decreased heat transmission and less heat intake to the air. When we examine the maximum output temperature at low and high flow rates, it drops from 64 ^{0}C to 51 ^{0}C. As illustrated in Fig. 13b. at a high airflow rate without a stainless tube, the maximum temperature difference reduces from 34.4 ^{0}C to 24 ^{0}C for low and medium flow

rate conditions. As shown in Fig. 13c. at a high flow rate without stainless steel tubes, it is observed that the maximum efficiency is found to be 18.6% at a solar intensity of 142 W/m^2.

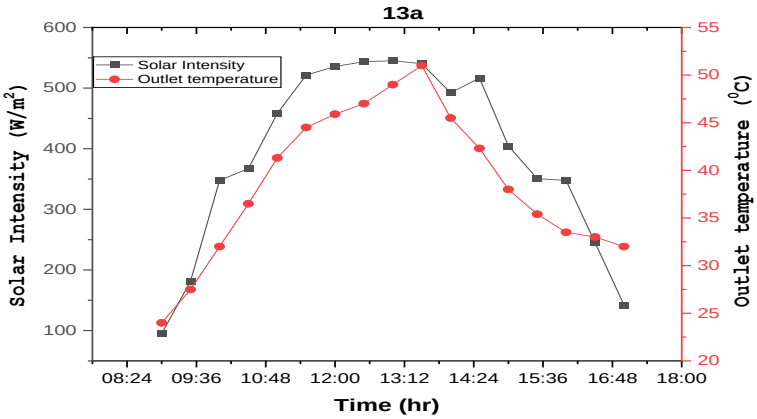

Fig. 13a Shows the daily variation in outlet temperature and solar intensity at a flow rate of 15.14 kg/h. Date 9th November 2022

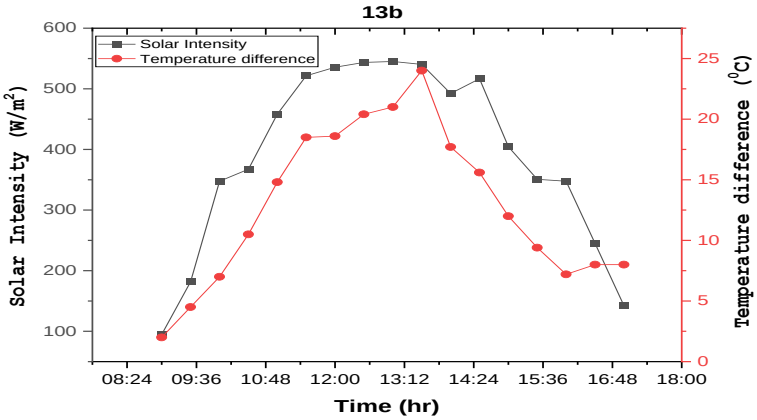

Fig. 13b Shows the daily efficiency and sun intensity variations at a flow rate of 15.14 kg/h. Date 9th November 2022

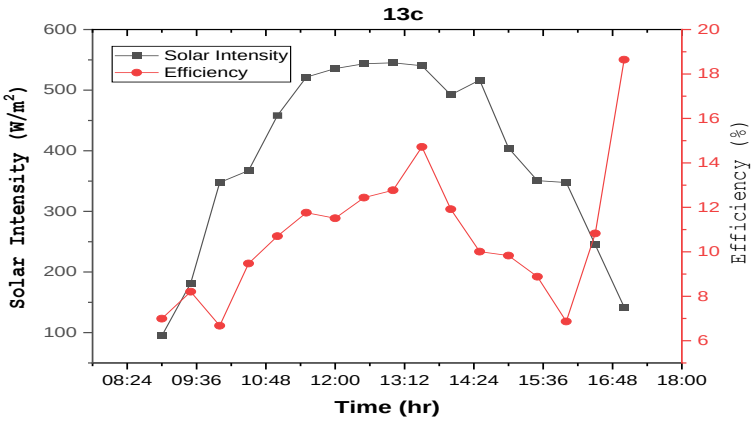

Fig. 13c shows the temperature difference and sun intensity variations at a flow rate of 15.14 kg/h. Date 9th November 2022.

5. Conclusions

The following findings were identified from the experiments:

- When all of the experimental results from the curve were compared, we discovered that the maximum temperature difference of 62.5^{0}C and maximum outlet temperature of 90.5 ^{0}C are obtained at a low flow rate of 4.58 kg/h when the directional inner stainless-steel tube of 20mm diameter and 1.27m length is fitted inside the evacuated tube with steel manifold channel.
- A comparison of all efficiency values for flow rates of 4.58kg/h, 9.16kg/h, and 15.14kg/h for different diameters of stainless-steel tubes. With a 20mm stainless tube diameter, the highest efficiency of 32.9% is attained at 15.14kg/h.

- When the diameter and mass flow rates are compared to efficiencies, temperature difference, and outlet temperature, it is observed that the efficiency, temperature difference, and outlet temperature rise with the diameter of the inner-fitted stainless tube.

Future Scope of the present work:

- Evacuated tube inner diameter and thickness are vital in maximizing the heat transfer rate because of the absorber's inner coating. The inner surface of the evacuated tube absorbs maximum heat, and finally, the heat transfer inside the tube occurs due to convection. Hence, if the inner diameter reduces the heat transfer rate while simultaneously increasing the convective heat transfer coefficient, the efficiency and effectiveness of the ETSCs can be enhanced by a certain percentage.

Acknowledgments

The evacuated tube solar collector for the project is fabricated in the Glocal University, Saharanpur, UP, in consultation with the research and development section.

Nomenclature

C_v	*specific heat capacity of water [J/kg K]*
m	*mass of water [kg]*
A_c	*area of evacuated tube solar collector [m^2]*
I	*intensity of solar radiation [W/m^2]*
D	*diameter of the evacuated tube [m]*
L	*length of the evacuated tube [m]*
d	*diameter of stainless-steel tube [m]*
G	*total radiant incident energy*
h_r	*radiation heat transfer coefficient [W/m^2K]*
h_c	*convection heat transfer coefficient [W/m^2K]*
T	*temperature [℃]*
v_∞	*ambient air velocity [m/s]*
Q_{in}	*heat supplied to the water [W]*
Q_{out}	*heat required by water [W]*

Subscript

w	*water*
∞	*ambient*
i	*inner glass tube*
ss	*stainless steel*
os	*outside diameter of stainless steel*
is	*internal diameter of stainless steel*
o	*outer glass tube*
og,i	*inner surface of the outer glass tube*
ig,i	*inner surface of the inner glass tube*
$g-\infty$	*between outer tube and ambient*
og,o	*outer surface of the outer glass tube*
ig,o	*outer surface of the inner glass tube*
s	*stainless steel*
ref	*reflection*
abs	*absorption*
trs	*transmission*
f	*final*
ini	*initial*
d	*difference*

Greek symbols

η	*collectorefficiency*
$\propto$	*absorptivity*
β	*tilt angle*
γ	*reflectivity*
$\in$	*emissivity*
ρ	*density*
τ	*transmissivity*
σ	*Stefan Boltzmann constant [W/m^2]*

Abbreviation

PCM	*Phase change material*
FPC	*Flat plate collector*
PV	*Photo voltaic*
ETSAC	*evacuated tube solar air collector*
ETSC	*evacuated tube solar collector*

Reference:

1) N. Kumari, S. Kumar Singh, S. Kumar, "Matlab-based simulation analysis of the partial shading at different locations on series-parallel PV array configuration", *Evergreen. Joint Journal of Novel Carbon Resource Sciences & Green Asia Strategy,* 9(4), 1126-1139, (2022). https://doi.org/10.5109/6625724

2) Saleh Abo-Elfadl, Hamdy Hassan, M.F. El-Dosoky, "Energy and exergy assessment of integrating reflectors on thermal energy storage of evacuated tube solar collector-heat pipe system", *Solar Energy, 209(June), 470–484. (2020).* https://doi.org/10.1016/j.solener.2020.09.009

3) M.S. Abd-Elhady, M. Nasreldin, M.N. Elsheikh, "Improving the performance of evacuated tube heat pipe collector using oil and foamed metals", *Ain Shams Engineering Journal, 9(4), 2683–2689.(2017).*

4) Avadhesh Yadav and V.K. Bajpai, "Comparison of flat plate and evacuated tube solar air collector thermal performances at different flow rates: an experimental analysis", *International Journal of Renewable Energy Technology*, *4*(2), 107. https://doi.org/10.1504/ijret.2013.052924

5) A. S. Olcha, T.Cholewa, & K.D.Howoruszko, "Experimental studies of thermal performance of an

evacuated tube heat pipe solar collector in Polish climatic conditions",*Environmental Science and Pollution Research*. https://doi.org/10.1007/s11356-020-07920-3(2020).

6) M.Ersoz, "Effects of different working fluid use on the energy and exergy performance for evacuated tube solar collector with thermosyphon heat pipe." *Renewable Energy, 96, 244–2(2016)*
7) Y.D.Kim, K.Thu, K.Choon Ng, "Evaluation of parametric optimization of the thermal performance and cost-effectiveness of active-indirect solar hot water plants*", Evergreen. Joint Journal of Novel Carbon Resource Sciences & Green Asia Strategy,* 2(2), 50-60, (2015). https://doi.org/10.5109/1544080
8) Ge, T. S., Wang, R. Z., Xu, Z. Y., Pan, Q. W., Du, S.Chen, X. M., Ma, T., Wu, X. N., Sun, X. L. & Chen, J. F. (2018). "Solar heating and cooling: Present and future development", *Renewable Energy*, *126*, 1126–1140. https://doi.org/10.1016/j.renene.2017.06.081
9) A.Kumar, S.Kumar, & A.Yadav, "Thermal performance analysis of evacuated tubes solar air collector in Indian climate conditions", *International Journal of Ambient Energy*, *37*(2), 162–171. *(2016).* https://doi.org/10.1080/01430750.2014.915884
10) K. Tewari, and R. Dev, "Analysis of modified solar water heating system made of transparent tubes & insulated metal absorber", *Evergreen Joint Journal of Novel Carbon Resource Sciences & Green Asia Strategy*, 5(1), 62–72, (2018). https://doi.org/10.5109/1929731
11) S.Kumar, A.Kumar, & A.Yadav, "Experimental analysis of the thermal performance of evacuated tube and flat-plate solar air collectors at different air flow rates", *International Journal of Sustainable Engineering*, *8*(4–5), 280–293. *(2015).* https://doi.org/10.1080/19397038.2013.878001
12) N.Mehla & A.Yadav, "Experimental nalysis of the thermal performance of evacuated tube solar air collector with phase change material for sunshine and off-sunshine hours", *International Journal of Ambient Energy, 38(2), 130145.(2017)* https://doi.org/10.1080/01430750.2015.1074612
13) E. Zambolin & D.D. Col, "An improved procedure for the experimental characterization of optical efficiency in evacuated tube solar collectors", *Renewable Energy, 43, 37–46. (2012)* https://doi.org/10.1016/j.renene.2011.11.01115.
14) P. Feliński & R.Sekret, "Experimental study of evacuated tube collector/storage system containing paraffin as a PCM",*Energy*, *114*, 1063–1072. (2016) https://doi.org/10.1016/j.energy.2016.08.057
15) L. Ma, Z. Lu, J. Zhang & R. Liang, "Thermal performance analysis of the glass evacuated tube solar collector with U-tube",*Building and Environment*, *45*(9), *1959–1967. (2010)* https://doi.org/10.1016/j.buildenv.2010.01.015
16) K.Chopra, A.K.Pathak, V.V. Tyagi, A.K. Pandey, S. Anand & & A. Sari, "Thermal performance of phase change material integrated heat pipe evacuated tube solar collector system : An experimental assessment",*Energy Conversion and Management*, *203, (2020)* https://doi.org/10.1016/j.enconman.2019.112205
17) W. N. Septiadi, K. Astawa, I. G. A.Pristha Arvikadewi, D. Febraldo, G.J. Puriadi Putra, "Boiling Phenomenon of Graphene Nano-Coating Wick Heat Pipe", *Evergreen Joint Journal of Novel Carbon Resource Sciences & Green Asia Strategy,* 7(2), 297-302, (2020). https://doi.org/10.5109/4055236
18) S. Singh, R.S. Gill, R. S, V.S.Hans, & T.C. Mittal, "Experimental performance and economic viability of evacuated tube solar collector assisted greenhouse dryer for sustainable development",*Energy*, *241*, *122794. (2022).*
19) Y. Kim & T. Seo, "Thermal performance comparisons of the glass evacuated tube solar collectors with shapes of the absorber tube", *Renewable Energy*, *32*(5), 772–795.(2006) https://doi.org/10.1016/j.renene.(2006).
20) M. K. Barai, B. B Saha, "Energy Security and Sustainability in Japan," *Evergreen: Joint Journal of Novel Carbon Resource Sciences & Green Asia Strategy,* 2(1), 49-56, (2015). https://doi.org/10.5109/1500427
21) P. Stevens, P.Tatsidjodoung, N. L. Pierrès, & L. Luo, "Modeling of a Coaxial Vacuum Solar Tube Collector", *(2013).* https://www.researchgate.net/publication/26263925214
22) S. Pandey, S.K. Mishra, A. Sharma, A.K.Verma, & L. Yadav, "Performance analysis of evacuated tube type solar air heater with parabolic trough type collector", *International Journal of Energy and Water Resources*, *6*(3), 337–*351. (2022)* https://doi.org/10.1007/s42108-021-00158-w
23) S.E. Zubriski & K.J. Dick, "Measurement of the efficiency of evacuated tube solar collectors under various operating conditions", *Journal of Green Building*, 7(3), 114–130. (2012). https://doi.org/10.3992/jgb.7.3.114
24) I. George & R. Kalaivanan, "Analysis of thermal performance on evacuated tube solar collector without and with reflector", 55–61. *(2017).* https://doi.org/10.1016/j.energy.2021.122794
25) Mohammadkarim, A. Kasaeian, A. Kaabinejadian, "Performance Investigation of Solar Evacuated Tube Collector Using TRNSYS in Tehran", *INTERNATIONAL JOURNAL of RENEWABLE ENERGY RESEARCH, Vol.4, No.2, (2014).*
26) S.Kaushik, V. Uniyal, A. k. Verma, A. Kumar Jha , oshi , M. Makhloga, P. Singh Pargai , S.K.Sharma R. Kumar , S. Pal, "Comparative Experimental and, CFD Analysis of Fluid Flow Attributes in Mini Channel with Hybrid CuO+ZnO+H2O Nano Fluid

and (H2O) Base Fluid", *EVERGREEN Joint Journal of Novel Carbon Resource Sciences & Green Asia Strategy*, 10(1), 182-195, (2022). https://doi.org/10.5109/6781069.

27) A. Dhiman, G.Sachdeva , "Energy and Exergy Analysis of a Pressurized Solar Cooking System Based on a Parabolic Dish Collector", *EVERGREEN Joint Journal of Novel Carbon Resource Sciences & Green Asia Strategy*, 9(4), 1168-1180, (2022). https://doi.org/10.5109/6625728
28) I. Singh, S. Vardhan, "Experimental investigation of an evacuated tube collector solar air heater with helical inserts*", Renewable Energy, Volume 163, Pages 1963-1972, (2021)*
29) Ayman I. Bakry , Y.A.F. EL-Samdony , S.A. El-gouz , A.M. Alshrombably , K.S. Abelfatah , M.A. S aid, "Performance of the one-ended evacuated tubes as medium temperature solar air heaters at low flow rates", *Sustainable Energy Technologies and Assessments Volume 30, Pages 174-182,(2018)*
30) Google map, 2023. Glocal University Mechanical Engineering Workshop [WWW Document]. URLhttps://www.google.com/maps/@30.2924954,77 .633596,1263m/data=!3m1!1e3!5m2!1e 4!1e2
31) https://world-weather.info/forecast/india/saharanpur/november-2022/